

Projective Reconstruction of General 3D Planar Curves from Uncalibrated Cameras

X.B. Zhang, A.W.K. Tang, and Y.S. Hung

Department of Electrical and Electronic Engineering,
The University of Hong Kong, Pokfulam Road, Hong Kong

Abstract. In this paper, we propose a new 3D reconstruction method for general 3D planar curves based on curve correspondences on two views. By fitting the measured and transferred points using spline curves and minimizing the 2D Euclidean distance from measured and transferred points to fitted curves, we obtained an optimum homography which relates the curves across two views. Once two or more homographies are computed, 3D projective reconstruction of those curves can be readily performed. The method offers the flexibility to reconstruct 3D planar curves without the need of point-to-point correspondences, and deals with curve occlusions automatically.

1 Introduction

Computer vision has been a hot topic in the past decades. While 3D reconstruction based on points or lines has been widely studied [1,2,3], 3D reconstruction methods based on curve correspondences have recently drawn the researchers' attention.

The existing literature of 3D reconstruction based on curve correspondences can be classified into three groups: conic reconstruction, high-order curve reconstruction and general 3D curve reconstruction. Among these three groups, the most restrictive one is based on projected conics [4,5,6,7] which, however, has attracted much more attention than the other groups.

Another group is high-order planar curve reconstruction provided by Kaminiski and Shashua. They suggested a closed form solution to the recovery of homography matrix from a single pair high-order curve matched across two views and the recovery of fundamental matrix from two pairs of high-order planar curves [8]. They have also extended this high-order method to general 3D curve reconstruction [9].

The last group is general 3D curve reconstruction from 2D images using affine shape. Berthilsson et al. [10] developed an affine shape method and employed it together with parametric curve for 3D curve reconstruction which demonstrated excellent reconstruction results. While this method is quite applicable, the minimized quantity is the subspace error, which lacks geometric meaning.

In this paper, we proposed a new method of general 3D planar curve reconstruction which solves for the homography between two views by minimizing the sum of squares of Euclidean distances from 2D measured and transferred points

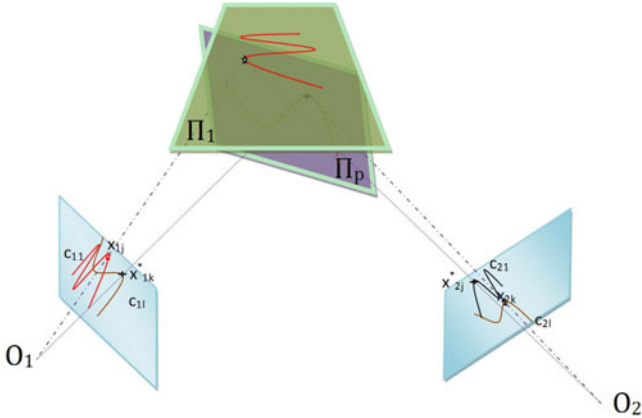


Fig. 1. Projective reconstruction of general curves

to fitted curves. Once 2 or more non-coplanar 3D planar curves are computed, 3D reconstruction for those two views can be readily performed. The curves visible on the two views are not required to be exactly the same portions of the 3D curve, hence the problem of occlusion can be handled. The paper is organized as follows: in Section II, the problem of reconstructing general 3D planar curves is formulated. In Section III, the details of the method is presented, together with the explanation of the algorithm. Experimental results are given in Section IV. In Section V, some concluding remarks are made.

2 Problem Formulation

Suppose that there are m general 3D curves C_l ($l = 1, 2, \dots, m$) lying on P ($P \leq m$) 3D planes Π_p ($p = 1, 2, \dots, P$). Each 3D curve can be seen by at least two views (in this paper, we will only consider 2-view cases but the approach can be extended to multi-views). For the l th 3D curve, the sets of 2D measured points on the first and second views are denoted as $\{x_{1l}\}$ and $\{x_{2l}\}$ respectively. Let $x_{il} = [u_{il}, v_{il}, 1]^T$ ($i = 1, 2$). Note that the index l doesn't indicate point-to-point correspondence between the two sets.

The projections on the two views of a 3D plane Π_p are related by a 3×3 non-singular homography, H_p . Suppose C_l is on Π_p . The set of 2D points $\{x_{2l}\}$ can be transformed to the first view as:

$$x_{1l}^* \sim H_p x_{2l}. \quad (1)$$

where \sim means equivalence up to scale.

The above relationship can be written into an equation by introducing a set of scale factors $\{\lambda_{2l}\}$:

$$\frac{1}{\lambda_{2l}} x_{1l}^* = H_p x_{2l}. \quad (2)$$

Let the projections of the 3D curve C_l on the first and second view be c_{1l} and c_{2l} respectively. The measured points $\{x_{1l}\}$ should ideally lie on c_{1l} ; and since $\{x_{2l}\}$

should lie on c_{2l} which corresponds to c_{1l} , the transferred points $\{x_{1l}^*\}$ should also lie on c_{1l} . Hence, we can obtain the set of curves $\mathbf{c} = \{c_{11}, c_{12}, \dots, c_{1m}\}$ by fitting them to both the measured and transferred points through the minimization problem:

$$E = \min_{\mathbf{H}, \mathbf{c}} \left(\sum_{l=1}^m d(x_{1l}, c_{1l})^2 + \beta \sum_{p=1}^P \sum_{l=1}^m d(\lambda_{2l} H_p x_{2l}, c_{1l})^2 \right). \quad (3)$$

subject to

$$\lambda_{2l} H_p^3 x_{2l} = 1. \quad (4)$$

where $d(x, c)$ is the Euclidean distance from point x to curve c ; β is a weighting factor in $[0, 1]$ and H_p^i is the i th row of the homography matrix H_p .

From (3), we can see that homographies are constrained by the second term while curve fitting relies on both of the terms. By setting a small β at the beginning and increasing it step by step (i.e. β takes value from set $\{\beta : \beta = 1 - e^{-n/a}, n \in \mathbb{N}, a = \text{const}\}$), the influence of the second term on curve fitting can be properly controlled and thus it can deal with the possibly poorly chosen initial homographies.

Instead of solving (3) directly with rigid constraint (4), we relax it to an unconstrained Weighted Least Square (WLS) problem by introducing a weighting factor γ to control the minimization problem from minimizing algebraic error to geometric error as γ increases. The relationship between algebraic error and geometric error is given in [1]. γ_{2l} are added as constant weighting factors [1]. Then the relaxed cost function could be written as:

$$E = \min_{\mathbf{H}, \mathbf{c}} \left\{ \sum_{l=1}^m d(x_{1l}, c_{1l})^2 + \beta \sum_{p=1}^P \sum_{l=1}^m \left(d(\lambda_{2l} H_p x_{2l}, c_{1l})^2 + \gamma \gamma_{2l} (1 - \lambda_{2l} H_p^3 x_{2l})^2 \right) \right\}. \quad (5)$$

The fitted curves on the first view together with optimized homographies provide one-to-one point correspondence along each curve across the two views, and thus facilitate stratified approach for projective reconstruction.

3 Projective Reconstruction

In this section, we will show how the problem can be reformulated into a multilinear WLS problem which can be solved by an iterative algorithm.

3.1 Spline Curve Construction

According to the definition of the B-spline, a B-spline curve is defined by its order, knot vector and control points. We employ cubic spline for approximating c_{1l} in our algorithm, so the order of spline curve is four in this paper. To further simplify the problem, we use a uniform knot vector in the range of $[0, 1]$, leaving the spline curve to be totally determined by its control points which can be updated iteratively.

3.2 Cost Function for Minimization Algorithm

In Section 2, we have already formulated the problem of projective reconstruction into a minimization problem, as shown in (5). In this part we will rewrite it into a cost function which is suitable for minimization implementation. The following notation is used to describe our newly developed cost function:

- $\mathbf{B}_{lj}(t)$ is the j th spline basis for curve c_{1l} .
- w_{lj} is the j th control point of curve c_{1l} .
- $G_{1l}(t) = \sum_j w_{lj} \mathbf{B}_{lj}(t)$ is the spline description of curve c_{1l} .
- $\{t_{1l}\}$ and $\{t_{2l}\}$ are sets of corresponding parametric values of measured point set $\{x_{1l}\}$ and transferred point set $\{x_{2l}\}$.
- $\mathbf{H} = \{H_1, H_2, \dots, H_P\}$ is the homography set of P 3D planes.
- $\mathbf{w} = \{w_{lj}, l = 1, 2, \dots, m\}$ is the set of control points of all spline curves.
- $\mathbf{t} = \{t_{11}, t_{12}, \dots, t_{1m}, t_{21}, t_{22}, \dots, t_{2m}\}$ is the set of all corresponding parametric values on the spline curves.
- $\lambda = \{\lambda_{21}, \lambda_{22}, \dots, \lambda_{2m}\}$ is the set of homography scaling factors of all transferred points.

The cost function is written as follows:

$$F_c(\mathbf{H}, \mathbf{w}, \mathbf{t}, \lambda, \beta, \gamma) = \sum_{l=1}^{l=m} \|x_{1l} - G_{1l}(t_{1l})\|^2 + \beta \sum_{p=1}^P \sum_{l=1}^m \left\{ \|\lambda_{2l} H_p x_{2l} - G_{1l}(t_{2l})\|^2 + \gamma \gamma_{2l} (1 - \lambda_{2l} H_p^3 x_{2l})^2 \right\}. \quad (6)$$

In (6), when β is small (i.e. $\beta \rightarrow 0$), the influence of the second term on curve fitting will be small so that the curve fitting is faithful to the original measured points of the first view; when $\beta \rightarrow 1$, the cost function has equal weights with regard to the points measured on the first view and those transferred from the second view. This automatically solves the curve occlusion problem. Also, when γ is small (i.e. $\gamma = 1$), the algebraic error between the transferred point and its corresponding point on the curve is minimized; whereas when $\gamma \rightarrow \infty$, the algebraic error becomes the geometric distance from the measured and transferred points to the curves.

3.3 Algorithm Initialization

One of the main advantages of this method is its flexibility of initialization: no point correspondences are needed to be known for this algorithm. However, three initializations must be done for the algorithm to start with. They are determining the first view, estimating the initial homographies and constructing the initial spline curves.

To determine the first view, one suggested strategy is to calculate the arc-length and the enclosed area of each curve (for open curves, connect the start and end points to estimate its area); and take the view with the smallest arc-length to area ratio as the first view.

In the literature, there are a number of methods to estimate the affine transformation between two point-sets, Fitzgibbon [11] suggested an improved Iterative Closest Point (ICP) algorithm which can be used to generate satisfactory initial homographies for our algorithm even there are missing data.

To deal with initial spline curves, we use split-merge algorithm, which is effective in not only determining the number of control points to be used but also providing the initial locations of control points.

3.4 Algorithm for Projective Reconstruction

As stated in Section 2, we are given m pairs of general curves on two views projected from P ($P \geq 2$) 3D planes. The curves on the two views are described as measured points $\{x_{1l}\}$ and $\{x_{2l}\}$, thus $\{x_{1l}\}$ and $\{x_{2l}\}$ in the cost function are already known. As the order of the spline curve is chosen to be four in this paper, the basis $\mathbf{B}_{lj}(t)$ is also determined considering that we have already set the knot vector to be uniform. Thus for fixed β and γ , when we keep \mathbf{t} fixed, the cost function $F_c(\mathbf{H}, \mathbf{w}, \mathbf{t}, \lambda, \beta, \gamma)$ is tri-linear with regard to the homographies \mathbf{H} , the control points \mathbf{w} and the homography scaling factors λ , which could be minimized with standard WLS method; when \mathbf{H} , \mathbf{w} and λ are fixed, minimizing $F_c(\mathbf{H}, \mathbf{w}, \mathbf{t}, \lambda, \beta, \gamma)$ becomes a geometric problem which is to find the nearest points on its corresponding spline curves $G_{1l}(t)$ and can easily be solved in an analytical way; consequently, the cost function F_c can be minimized by iteratively finding the optimums of \mathbf{H} , \mathbf{w} , λ and \mathbf{t} . When β and γ are increasing, the minimized cost function is going from the algebraic error to the geometric error. Thus the equation (6) generates optimum solution \mathbf{H}^* , \mathbf{w}^* , \mathbf{t}^* and λ^* by minimizing the geometric distance from measured and transferred points to fitted curves. Once optimal \mathbf{H} , \mathbf{w} , \mathbf{t} and λ are obtained, the fundamental matrix F relating the two views can be retrieved by either using the homographies [12] or employing the eight-point algorithm [13] with the optimal corresponding points. And the projection matrix can be written as [14]:

$$P_1 = [\mathbf{I}_{3 \times 3}, \mathbf{0}_{3 \times 1}]. \quad (7)$$

$$P_2 = [[e']_{\times} F, e']. \quad (8)$$

where e' is the epipole on the second view.

With the projection matrix and one-to-one point correspondence along the curves, the 3D projective reconstruction can be readily performed. The algorithm is described as follows:

Algorithm 1

1. Initialization

Put $k = 0$ and set $\beta^{(0)} = 0, \gamma^{(0)} = 1$;

Initialize $\mathbf{H}^{(0)}$ and $\mathbf{w}^{(0)}$ according to the strategies described in Section 3.3.

2. Put $k = k + 1$

3. Fix $\mathbf{H}^{(k-1)}$, $\mathbf{w}^{(k-1)}$ and $\lambda^{(k-1)}$, determine t_{1l} and t_{2l} by solving:

$$err'_k = \min_{\mathbf{t}^{(k)}} F_c \left(\mathbf{H}^{(k-1)}, \mathbf{w}^{(k-1)}, \mathbf{t}^{(k-1)}, \lambda^{(k-1)}, \beta^{(k-1)}, \gamma^{(k-1)} \right). \quad (9)$$

4. Fix $\mathbf{w}^{(k-1)}, \mathbf{t}^{(k)}$ and $\lambda^{(k-1)}$, find $\mathbf{H}^{(k)}$ by solving

$$err_k'' = \min_{\mathbf{H}^{(k)}} F_c \left(\mathbf{H}^{(k)}, \mathbf{w}^{(k-1)}, \mathbf{t}^{(k)}, \lambda^{(k-1)}, \beta^{(k-1)}, \gamma^{(k-1)} \right). \quad (10)$$

5. Fix $\mathbf{H}^{(k)}, \mathbf{w}^{(k-1)}$ and $\mathbf{t}^{(k)}$, determine $\lambda^{(k)}$ by solving:

$$err_k''' = \min_{\lambda^{(k)}} F_c \left(\mathbf{H}^{(k)}, \mathbf{w}^{(k-1)}, \mathbf{t}^{(k)}, \lambda^{(k)}, \beta^{(k-1)}, \gamma^{(k-1)} \right). \quad (11)$$

6. Fix $\mathbf{H}^{(k)}, \mathbf{t}^{(k)}$ and $\lambda^{(k)}$, find $\mathbf{w}^{(k)}$ by solving:

$$err_k = \min_{\mathbf{w}^{(k)}} F_c \left(\mathbf{H}^{(k)}, \mathbf{w}^{(k)}, \mathbf{t}^{(k)}, \lambda^{(k)}, \beta^{(k-1)}, \gamma^{(k-1)} \right) \quad (12)$$

7. If $|err_k - err_k'| \geq \varepsilon$ (e.g. $\varepsilon = 10^{-4}$), increase β ; else increase γ by $\gamma = 1.1\gamma$.

8. If $k \leq N$ and $\gamma \leq M$ (e.g. $M = 10000, N = 1000$), go to Step 2.

9. Compute the fundamental matrix F using the optimized homographies or new point-to-point correspondences.

10. Compute the projection matrix according to (7) and (8). Output projection matrix P_1 and P_2 .

11. End

The reconstructed curves in a projective 3D space can be upgraded to Euclidean space by enforcing metric constraints on the projection matrices, as proposed by Tang [15].

4 Experimental Results

To demonstrate the performance of our proposed method, both synthetic data and real images are tested in this section.

4.1 Synthetic Data

A synthetic scene is given in Fig. 2(a), which consists of two general curves on two orthogonal planes in 3D space: the blue one is a sine function while the red one is a high-order curve, defined as:

$$\begin{cases} z = 6 \sin(y) \\ x = 0 \end{cases}, \quad y \in [-2\pi \ 2\pi] \quad (13)$$

and

$$\begin{cases} z = 3.5 \times 10^{-4} (x^2 - 25)^3 + 1 \\ y = 0 \end{cases}, \quad x \in [-7.5 \ 7.5] \quad (14)$$

Curves are projected on two views by two cameras at randomly generated locations with focal length 340 and image size 320×320 .

Along each of the projected curves on both of the views, 200 points are sampled randomly; then Gaussian noise with standard deviation 1 pixel is added

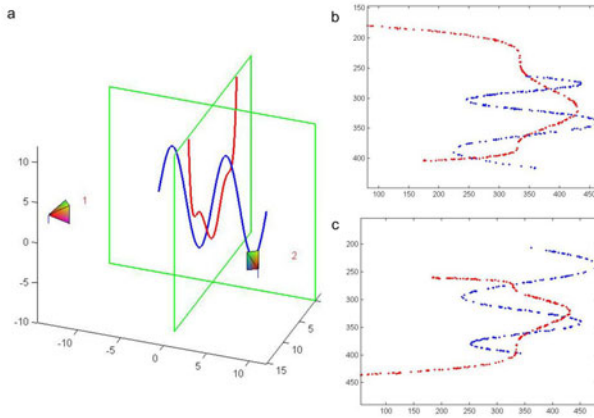


Fig. 2. The synthetic scene together with two synthetic views. (a) The 3D scene used to evaluate the performance of the proposed algorithm. (b) The view taken by camera one. (c) Another view taken by camera two.

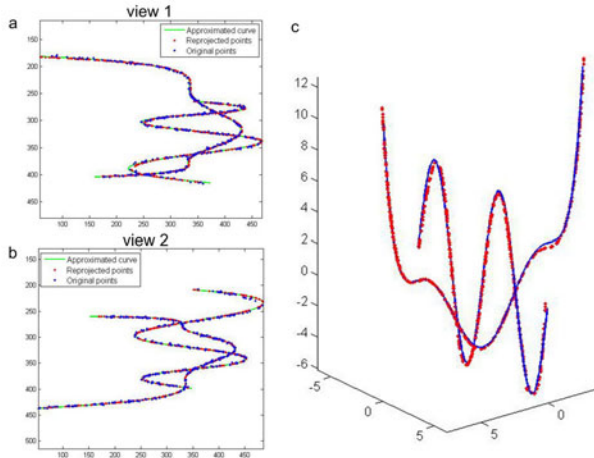


Fig. 3. The reconstruction results. (a) The approximation of curves on view one, where the black dots are measured points on view one; the red dots are transferred points from view two; the green lines are approximated curves. (b) the approximation of curves on view two, with same notation as in (a). (c) 3D reconstruction of measured points upgraded to Euclidean space and super-imposed with ground truth curves.

independently to both the x - and y -coordinates of those points on both of the views, as shown in Fig. 2(b) and (c).

The estimated curves on the first and second view together with reprojected measured points are shown in Fig. 3(a) and (b) respectively. The upgraded reconstruction result is shown in Fig. 3(c). We can see from the result that the reconstructed points lie quite close to that of the ground truth curves,

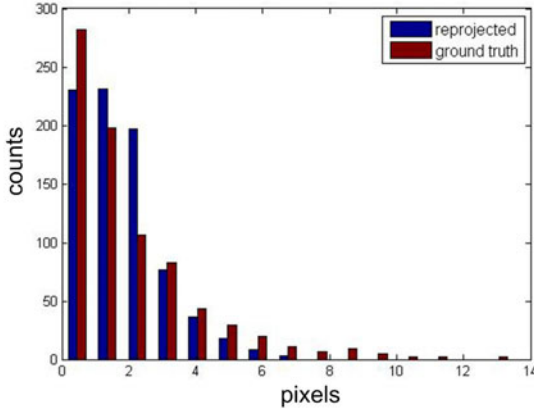


Fig. 4. The histogram comparison of noise distributions: the brown bars indicate the ground truth distribution. While the blue ones indicate the distance of measured points to reprojected curves.

indicating that our algorithm converges to the right solution. Also, from the point to reprojected curve distance shown in Fig. 4, we can see that the reconstructed point-to-curve error is quite close to that of the ground truth distribution of added noise in the simulation.

4.2 Real Image Curves

The proposed algorithm is also checked with real image curves. Two images of printed pictures of an apple and a pear are taken at two different positions, as shown in Fig. 5(a) and (b). Curves on these images are extracted with canny

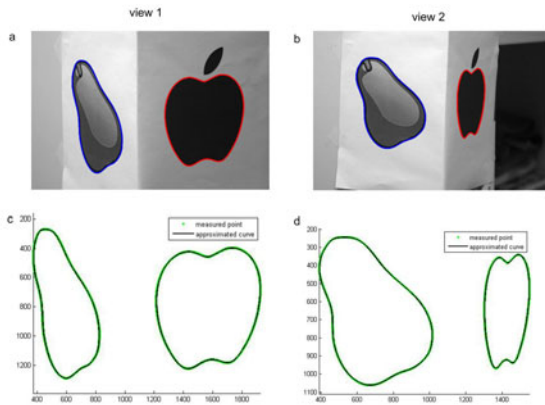


Fig. 5. (a) and (b) Two images of the printed picture taken at two different positions. (c) and (d) Extracted edge points and fitted curves on views one and two.

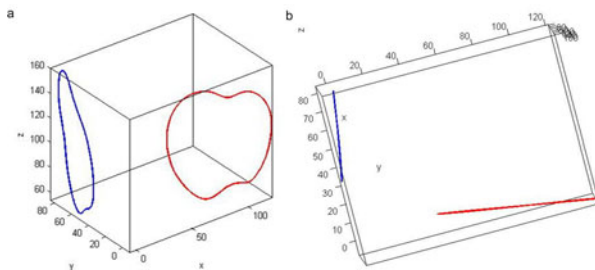


Fig. 6. (a) The reconstructed scene of real images. (b) A top view of the reconstruction result.

edge detector to generate the measured points on the curves. These extracted curves are then processed using our proposed algorithm until it converges, outputting the projection matrix for projective reconstruction. Finally, the results are upgraded to Euclidean space, as shown in Fig. 6.

5 Conclusion

In this paper, a new approach is developed to reconstruct general 3D planar curves from two images taken by uncalibrated cameras. By minimizing the sum of squares of Euclidean point to curve distances, we retrieve the curves on the first view and obtain an optimum homography matrix, thus established one-to-one point correspondences along the curves across the two views. With curves lying on more than one 3D plane, the fundamental matrix are computed, allowing the 3D projective reconstruction to be readily performed.

References

1. Hung, Y.S., Tang, A.W.K.: Projective reconstruction from multiple views with minimization of 2D reprojection error. *International Journal of Computer Vision* 66, 305–317 (2006)
2. Tang, A.W.K., Ng, T.P., Hung, Y.S., Leung, C.H.: Projective reconstruction from line-correspondences in multiple uncalibrated images. *Pattern Recognition* 39, 889–896 (2006)
3. Hartley, R.I.: Projective reconstruction from line correspondences. In: *IEEE Computer Society Conference on Computer Vision and Pattern Recognition* (1994)
4. Long, Q.: Conic reconstruction and correspondence from two views. *IEEE Transactions on Pattern Analysis and Machine Intelligence* 18, 151–160 (1996)
5. Ma, S.D., Chen, X.: Quadric reconstruction from its occluding contours. In: *Proceedings International Conference of Pattern Recognition* (1994)
6. Ma, S.D., Li, L.: Ellipsoid reconstruction from three perspective views. In: *Proceedings International Conference of Pattern Recognition* (1996)
7. Mai, F., Hung, Y.S., Chesi, G.: Projective reconstruction of ellipses from multiple images. *Pattern Recognition* 43, 545–556 (2010)

8. Kaminski, J., Shashua, A.: On calibration and reconstruction from planar curves. In: Vernon, D. (ed.) ECCV 2000. LNCS, vol. 1842, pp. 678–694. Springer, Heidelberg (2000)
9. Kaminski, J.Y., Shashua, A.: Multiple view geometry of general algebraic curves. *International Journal of Computer Vision* 56, 195–219 (2004)
10. Berthilsson, R., Astrijm, K., Heyden, A.: Reconstruction of general curves, using factorization and bundle adjustment. *International Journal of Computer Vision* 41, 171–182 (2001)
11. Fitzgibbon, A.W.: Robust registration of 2D and 3D point sets. *Image and Vision Computing* 21, 1145–1153 (2003)
12. Luong, Q.T., Faugeras, O.D.: The fundamental matrix: Theory, algorithms, and stability analysis. *International Journal of Computer Vision* 17, 43–75 (1996)
13. Hartley, R.I.: In defense of the eight-point algorithm. *IEEE Transactions on pattern analysis and machine intelligence* 19, 580–593 (1997)
14. Hartley, R., Zisserman, A.: *Multiple view geometry in computer vision*. Cambridge University Press, Cambridge (2000)
15. Tang, A.W.K.: A factorization-based approach to 3D reconstruction from multiple uncalibrated images. Ph.D. Dissertation (2004)